Synthesis, Structure, and Electrical Properties of Ta_4FeTe_4

Jörg Neuhausen, Ernst Wolfgang Finckh, and Wolfgang Tremel*

Institut für Anorganische Chemie und Analytische Chemie, Universität Mainz
J.-J. Becherweg 24, D-55128 Mainz, FRG

Received September 1, 1994

Key Words: Early transition metal tellurides / Chain structure / Cluster compounds

Ta_4FeTe_4 has been synthesized and its structure determined by single-crystal X-ray methods. It crystallizes in the orthorhombic space group Pbam with $Z = 4$ and $a = 10.514(5)$, $b = 18.275(7)$, and $c = 4.815(1)$ Å. Ta_4FeTe_4 has a chain structure built up by Fe-centered Ta_8-square antiprisms sharing common square faces. The resistivity of Ta_4FeTe_4 has been measured by a two-point method. Ta_4FeTe_4 shows metallic behavior. The structure of Ta_4FeTe_4 is discussed in relation to other early transition metal cluster compounds. A rational approach to the synthesis of related compounds is proposed.

Introduction

Transition metal chalcogenides have been the subject of extensive investigation during the last decades. Their properties as well as their structural chemistry have attracted the interest of both physicists and chemists. For example, the transition metal dichalcogenides MX_2 (M = Nb, Ta; X = S, Se) show interesting structural phase transitions such as charge density waves[1], accompanied by anomalities in their physical properties[2], and a rich intercalation chemistry[3].

Another important class of transition metal chalcogenides are the molybdenum chalcogenides Mo_3X_4 (X = S, Se, Te) and their stuffed derivatives $M'_xMo_6S_8$ (M' = Pb, Sn, Fe, Co, Ni, Cu etc.), the so called Chevrel phases[4]. One interesting aspect of these materials is their superconductivity at high critical fields, in some cases accompanied by antiferromagnetic ordering[5]. The structure of the Chevrel phases is built up from octahedral Mo_6 clusters, where chalcogen atoms reside on top of the triangular faces of the octahedron. In compounds such as $M'Mo_3X_3$ (M' = Na, K, Rb, Cs, In, Tl; X = S, Se, Te) the clusters are condensed via common triangular faces to form an infinite chain[6]. Several binary and ternary tantalum and niobium chalcogenides with structures containing chains of metal clusters have been discovered so far. Chains of tricapped trigonal prisms have been found in $Ta_9M_2S_6$[7] and $Ta_{11}M_2Se_8$ (M = Fe, Co Ni)[8], whereas the structures of Ta_6S[9], Ta_2S[10], and Ta_3S_2[11] contain chains of Ta-centered pentagonal Ta_{10} antiprisms. Remarkably, chains of face-sharing Si-centered Ta_8 square antiprismatic clusters sheathed by tellurium atoms have been found in the structure of Ta_4SiTe_4[12]. Other members of a class of compounds M_4ZTe_4 (M = Nb, Ta; Z = Cr, Fe, Co, Ni, Al, Si) have been claimed to exist based on the results of X-ray powder diffraction, but none of them has been characterized[12]. A tight binding study of the electronic structure of Ta_4SiTe_4 indicates that a replacement of Si by Fe or Co may be possible[13]. Most recently, lattice constants for Ta_4ZTe_4 (Z = Si, Cr, Fe, Co) and Nb_4ZTe_4 (Z = Si, Fe, Co) derived from X-ray powder diffraction data have been given together with the results of electrical conductivity measurements for Ta_4ZTe_4 (Z = Si, Cr, Co) and Nb_4ZTe_4 (Z = Si, Fe, Co)[14]. Still, except for Ta_4SiTe_4 no single crystal structure investigations have been reported. In this paper we report on the synthesis, crystal growth and single crystal structure determination of Ta_4FeTe_4. The electrical properties of this compound are determined by two-point resistivity measurements.

Results

Ta_4FeTe_4 crystallizes in a chain structure. Slightly distorted square antiprisms, formed by tantalum atoms, sharing common square faces build up an infinite linear chain running parallel to the crystallographic c axis. Each Ta_8 antiprism is centered by an iron atom resulting in an infinite Fe chain running inside the Ta network. Tellurium atoms reside above the edges of each Ta_4 square so that the Te and Ta atoms lie in the same plane. A view of the structure along the c direction is shown in Figure 1.

The Ta_4FeTe_4 chains are arranged in the orthohombic unit cell in an approximately closest packed manner. The chains are held together by van der Waals interactions between the Te atoms as suggested by the Te–Te distances [shortest interchain Te–Te separation. 3.800(4) Å]. The intrachain Te–Te distances range from 3.850(4) to 3.894(4) Å indicating only weak Te–Te-interactions inside the chains as well.

Each Ta atom is coordinated by four Te atoms. Two of them lie at the same height in z direction, i.e. in the plane defined by the corresponding Ta_4 square, at an average Ta–Te distance of 2.842 Å. The remaining two Te atoms are located in planes built by the neighboring Ta_4 squares at an average Ta–Te distance of 2.917 Å. Thus, each Te atom bridges four Ta atoms, two of them belonging to one Ta_4 square, the remaining two being part of adjacent squares.

One characteristic feature of the Ta_4FeTe_4 structure are the numerous short metal-metal contacts. Each Ta atom has

  0009–2940/95/0606–0569 $ 10.00+.25/0

Figure 1. View of the Ta_4FeTe_4 structure along the crystallographic *c* axis (large dotted circles: Te; medium shaded circles: Ta; small open circles: Fe[a]

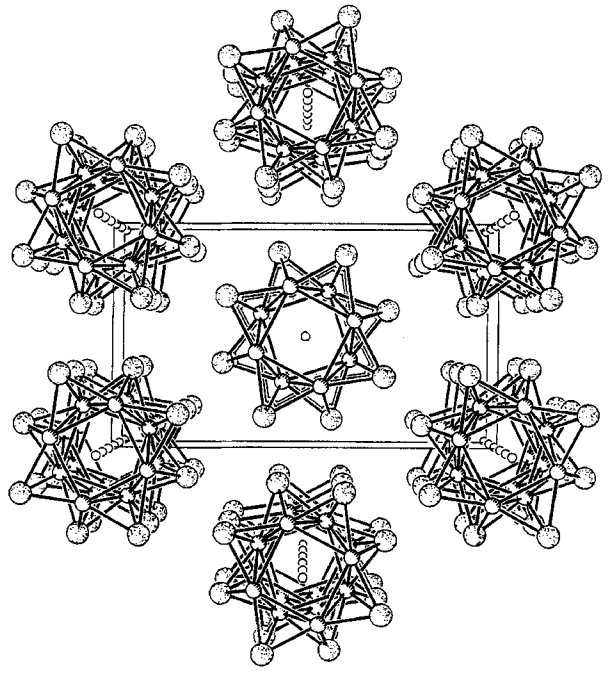

[a] Selected distances [Å]: Ta(1)–Ta(2) 2.892(2) (2 ×), Ta(1)–Ta(3) 3.252(3), Ta(1)–Ta(3) 3.291(3), Ta(1)–Ta(4) 2.995(2) (2 ×), Ta(2)–Ta(3) 2.986(2) (2 ×), Ta(2)–Ta(4) 3.265(3), Ta(2)–Ta(4) 3.279(3), Ta(1)–Fe 2.599(4) (2 ×), Ta(2)–Fe 2.619(4) (2 ×), Ta(3)–Fe 2.619(4) (2 ×), Ta(4)–Fe 2.595(4) (2 ×), Fe–Fe 2.40(1), Fe–Fe 2.41(1), Ta–Te distances in the range between 2.829(4)–2.924(2).

six Ta neighbors, two of them in the same Ta_4 square and four belonging to neighboring squares. The intrasquare Ta–Ta distances (average: 3.272 Å) are significantly longer than the intersquare ones (average: 2.989 Å).

The Fe atoms situated in the centers of the Ta_8 square antiprisms have contacts to eight Ta and two Fe atoms at average distances of 2.608 and 2.405 Å, respectively.

As expected for a metal-rich compound with partially filled d-bands and extensive metal-metal bonding Ta_4FeTe_4 shows metallic behavior between 8 and 275 K. As shown in Fig. 2, the specific resistivity decreases from 6.5 mΩcm at 275 K to 1.6 mΩcm at 8 K. No anomalities are observed in this temperature range.

Discussion

The Ta–Te distances ranging from 2.829(4) to 2.924(2) Å are comparable to those found in other tantalum tellurides [$TaTe_2$: d_{Ta-Te} = 2.818[15], $TaFe_{1.14}Te_3$: d_{Ta-Te} = 2.775–2.882 Å[16]]. The intersquare Ta–Ta distances range from 2.982(2) to 2.995(2) Å and are only slightly longer than those observed in Ta metal (2.86 Å)[17], whereas the intrasquare Ta–Ta distances [3.252(3)–3.291(3) Å] are significantly longer, but still short enough to be considered bonding. Strong metal-metal bonding is expected between Ta and Fe atoms based on their interatomic distances [d_{Ta-Fe} = 2.595(4)–2.619(4) Å]. These distances are considerably shorter than those found in other ternary tantalum-iron tellurides [$TaFe_{1.14}Te_3$: d_{Ta-Fe} = 2.859(1)–2.938(10) Å[16], $Ta_{0.77}Fe_{0.90}Te_2$: d_{Ta-Fe} = 2.667(2)–2.810(4) Å[18]] or molecular species such as $[TaFe_2S_4Cl_4]^{3-}$ [d_{Ta-Fe} = 2.842(8) Å][19]. The very short Fe–Fe distances of 2.40(1)–2.41(1] Å suggest strong interactions between neighboring Fe atoms as well. Typical Fe–Fe distances, e.g. in Fe metal (2.4823 Å)[17] or in most other ternary tantalum-iron tellurides showing substantial metal-metal bonding [$TaFe_{1.14}Te_3$: d_{Fe-Fe} = 2.4911(9)–2.715(1) Å, $Ta_{0.77}Fe_{0.90}Te_2$: d_{Fe-Fe} = 2.459(8) Å] are considerably longer, as are the Fe–Fe distances observed in iron-cluster compounds such as $Cs_7Fe_4Te_8$ (d_{Fe-Fe} = 2.846 Å)[20] or $[Fe_6Te_8(PEt_3)_6]$ (d_{Fe-Fe} = 2.65 Å)[21]. Only in $Ta_{1.09}Fe_{2.39}Te_4$ [d_{Fe-Fe} = 2.415(3)–2.538(5) Å][22] comparable Fe–Fe distances have been observed. As one might expect from the similarity of the atomic radii of Fe (1.25 Å) and Si (1.18 Å), the length of the repeat unit along the cluster chain is almost identical for Ta_4SiTe_4 and the corresponding Fe derivative. Interestingly, the Fe–Fe separations along the Ta_4FeTe_4 chain are almost identical [2.40(1) and 2.41(1) Å], whereas a weak bond alternation is observed for Ta_4SiTe_4 [2.35(2) and 2.45(2) Å][13]. This structural feature can be nicely correlated with the electrical properties of both materials. While Ta_4FeTe_4 is a simple metallic conductor, the resistivity behavior of Ta_4SiTe_4 suggest a semiconducting ground state that derives from a Peierls distortion[14].

Figure 2. Plot of the specific resistivity of Ta_4FeTe_4 versus temperature (cooling and heating cycle)

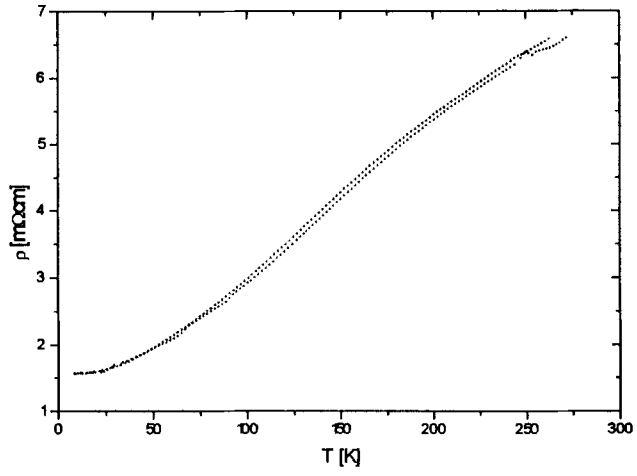

The planar Ta_4Te_4 unit (Figure 3a) observed in Ta_4FeTe_4 and Ta_4SiTe_4 can be regarded as a fragment of a M_6X_{12} cluster (Figure 3b). These clusters are known to constitute the main structural feature of many metal-rich compounds of the electron-deficient transition metals[23]. For example, the halides of niobium and tantalum in their lower oxidation states such as Nb_6Cl_{14}[24] or Ta_6Cl_{15}[25] contain such units. MO considerations show a valence electron concentration of 14 or 16 electrons per M_6 unit to be favorable for the formation of such clusters. If the halogen atoms are replaced by chalcogens the cluster electron count decreases. The resulting electron deficiency can be compensated by in-

Figure 3. Schematic representation of the assembly of hypothetical $Ta_{4n-6}Fe_nTe_{4n-12}$ fragments from planar Ta_4Te_4 units of Ta_4FeTe_4 (a) and a Ta_6Te_{12} cluster (b); successive insertion of Ta_4Te_4 units, including one interstitial Fe atom per unit, into a Ta_6Te_{12} cluster leads to the formation of $Ta_{4n+6}Fe_nTe_{4n+12}$ fragments [(c): $n = 1$, (d): $n = 2$, large circles: Te, medium circles; Ta, small circles: Fe, shaded atoms correspond to the inserted fragments]; note that a fragment with $n = 0$ is identical to the Ta_6Te_{12} cluster shown in Figure 3b, whereas $n = \infty$ corresponds to the infinite Ta_4FeTe_4 chain

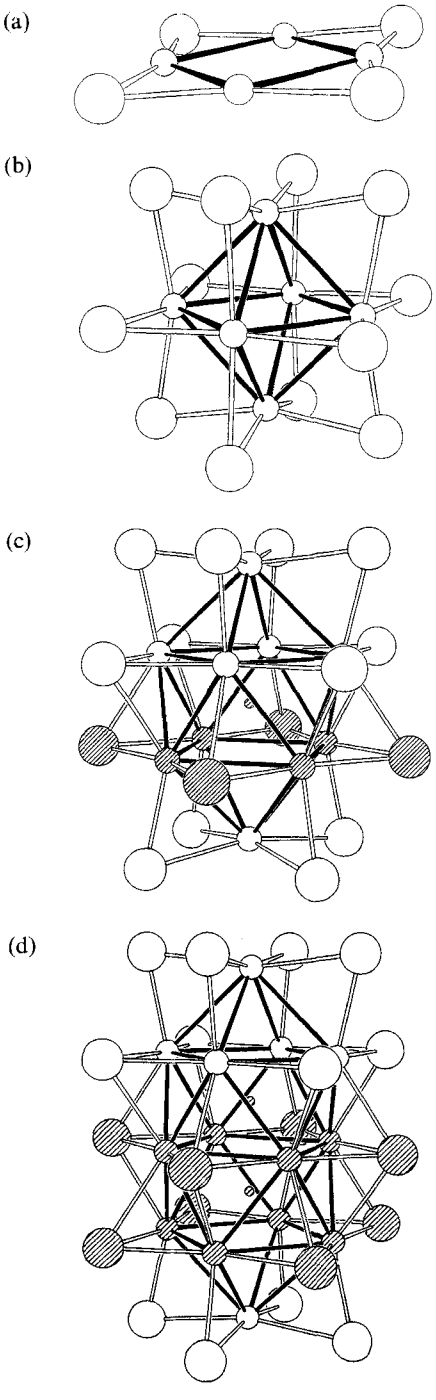

corporating small interstitial atoms into the clusters and/or by insertion of strongly electropositive elements between the clusters. The rich structural chemistry of the "reduced" oxoniobates and the rare earth halides[26] shows that variations of the electron concentration can induce various modes of cluster condensation as well. Indeed, the recent synthesis and characterization of Ta_4BTe_8[27], a compound containing chains of condensed Ta_6Te_{12} clusters stuffed with boron atoms, indicate that this concept may also be transferred to "reduced" tantalum tellurides.

In view of these facts the question arises, if Ta_4FeTe_4 is only the end member of a series of compounds containing (hypothetical) $Ta_{4n+6}Fe_nTe_{4n+12}$ units (Figures 3c and d) assembled from structural fragments of Ta_4FeTe_4 ($n = \infty$) and M_6X_{12} cluster compounds ($n = 0$). The geometric and electronic factors responsible for their stability do not preclude the existence of such units as indicated by the results of preliminary estimations. Similar fragments of linear cluster chains of the general composition $Mo_{3n}X_{3n+2}$ (X = chalcogen) are known to exist for Chevrel-type compounds, where the cluster size can be related to the valence electron concentration[28].

Adjustments of the cluster electron count are possible by intercalation of appropriate donor atoms between the clusters. A tight binding study of M_4ZTe_4 systems[13] shows the existence of an optimum valence electron count for M_4SiTe_4, where any increase of the valence electron concentration leads to a population of antibonding and any decrease to a depopulation of bonding states. The synthesis of $Nb_x[Nb_4GaTe_4]$ shows how adjustments of the valence electron concentration can be managed[29]. Here Nb atoms in the van der Waals gap between the cluster columns are used to compensate for the electron deficiency caused by the substitution of Ga for the Si interstitial. A replacement of Nb by other atoms of appropriate size such as Rb, Cs or Tl seems possible. Synthetic efforts to support this assumption are presently being made.

The present paper is part of the planned Ph. D. thesis of *J. Neuhausen* and *E. W. Finckh*. This work was supported by a grant of the *Bundesministerium für Forschung und Technologie* under contract 05 5UMGAB. Further support came from the *Deutsche Forschungsgemeinschaft (DFG)* and the *Fonds der Chemischen Industrie*. We are also grateful to Dr. *G. Höfer* (Heraeus Quarzschmelze) und Dr. *J. Peters* (H. C. Starck Co.) for generous gifts of quartz tubes and tantalum powder.

Experimental

Synthesis: Ta_4FeTe_4 can be prepared by heating the elements in the ratio 4:1:4 in sealed evacuated silica tubes in the temperature range from 700 to 1000 °C. Attempts to grow single crystals suitable for X-ray diffraction by transport reactions using iodine, $TeBr_4$ or $TeCl_4$ as transport agents failed. The needle-shaped crystals obtained by these reactions tended to be twinned or were too thin for single crystal structure investigations.

The crystal used in the single crystal study was prepared by reaction of Ta powder (Starck, 99.8%), Fe powder (Merck, 99,99%), Te powder (Aldrich, 99,8%), and Ta_2O_5 powder (Alfa, 99,5%). The starting materials were loaded into a silica tube (length approx. 10 cm, diameter 12 mm) in a ratio corresponding to the nominal composition Ta_4FeTe_4O. The tube was then evacuated to ca. 10^{-3} Torr, sealed, and placed in a tube furnace. The sample was kept at 500 °C for 2 d and then heated to 1000 °C. After 10 d the furnace was switched off. Very fragile needle-shaped crystals (up to

1 mm in length and 0.05 mm in diameter) showing metallic cluster formed throughout the tube.

Energy-dispersive analysis of X-rays using a Zeiss DSM 962 scanning electron microscope equipped with a Kevex analyzer performed on several crystals prepared by the different methods previously described uniformly gave a Ta:Fe:Te ratio of 4:1:4.

The X-ray powder patterns of samples prepared with and without addition of Ta_2O_5 are identical and the difference electron density map obtained in the structure refinement shows no peak that can be attributed to an oxygen atom. The presence of oxygen in the title compound cannot be completely ruled out based on the results of the structure refinements. However, chemical reasoning suggests that the insertion of oxygen close to the negatively charged Te surface of the cluster chain is unfavorable because of severe Coulomb repulsion. Furthermore, replacement of the interstitial Fe atoms by oxygen within the antiprismatic Ta_8 cluster should be detectable by X-ray diffraction. Finally, the presence of oxygen within the Ta_8 clusters can be ruled out based on size and bond length considerations[30]. Therefore, we assume that no oxygen is incorporated into the structure. The role of Ta_2O_5 in the growth of Ta_4FeTe_4 crystals is not yet understood.

The title compound is moderatly air-sensitiv. Finely dispersed samples often ignite in air, while large single crystals show only an oxygen attack at the surface when exposed to air for short times. During the three day X-ray data collection no significant decay of X-ray scattering was observed. However, after several weeks, the X-ray scattering power of the studied crystal decreased considerably.

Crystal-Structure Determination: The samples were examined by X-ray powder diffraction using an Enraf Nonius FR 552 Guinier camera (quartz added as an internal standard). The powder patterns obtained matched the theoretical patterns calculated by using the program LAZY-PULVERIX[31] and the atomic parameters obtained by the single-crystal structure refinement.

Single crystal studies were carried out on a needle-shaped crystal (approximate dimensions 0.2 × 0.03 × 0.02 mm) by using an automated Syntex $P2_1$ four-circle diffractometer equipped with a graphite monochromator (MoK_α radiation, $\lambda = 0.71073$ Å) and a scintillation counter.

Ta_4FeTe_4 exhibits orthorhombic symmetry. Lattice constants were obtained by least-squares refinement using the setting angles of 30 centered reflections in the range $15° < 2\theta < 30°$. Intensity data were collected by using the ω-scan technique. Three check reflections measured every 97 scans showed no significant deviation during data collection. Conventional atomic scattering factors were used and anomalous dispersion corrections were applied[32]. The data were empirically corrected for absorption effects by using the ψ-scan technique. Symmetry equivalent reflections were averaged. Details concerning the data collection are given in Table 1.

Table 1. Crystal data, structure determination and refinement parameters for Ta_4FeTe_4

Emp. formula: Ta_4FeTe_4; crystal needle-shaped, size: 0.2 × 0.03 × 0.02 mm; orthorhombic, space group *Pbam*; $a = 10.514(5)$, $b = 18.275(7)$, $c = 4.815(1)$ Å; $V = 925.2(7)$ Å^3; $Z = 4$; mol. mass: 1290.1 gmol^{-1}; $\rho_{calcd.} = 9.262$ gcm^{-3}; $\mu = 60.931$ mm^{-1}; radiation: Mo-K_α, $\lambda = 0.71073$ Å; temperature: 298 K; ω-scan, 2θ range: $4° \le 2\theta \le 54°$; $-13 \le h \le 0$, $-22 \le k \le 0$, $-6 \le l \le 6$; total reflections: 1894; independent reflections: 1065, of which 808 were observed [$I > 2\sigma(I)$]; absorption correction: ψ-scan (min./max. transmission: 0.4342/0.7161); Siemens SHELXTL PLUS (PC Version), direct methods, full-matrix least squares, extinction correction, 55 parameters, $R = 0.0536$, $R_w = 0.0574$ [$w = 1/\sigma^2(F_0) + 0.0001\,F_0^2$], GOF = 2.33; data-to-parameter ratio: 14.7:1; residual electron desity (min./max.): −4.46/4.34 e/Å^3

The structure was solved and refined by using the SHELXTL-Plus program package (Siemens Analytical X-ray Instruments). Analysis of the systematic extinctions led to the possible space groups *Pbam* (No. 55) and *Pba2* (No. 32). The distribution of normalized structure factors indicated a centrosymmetric structure with space group *Pbam*. This choice was confirmed by successful structure refinement in this space group. Direct methods gave the approximate positions of all nine crystallographically independent atoms. The structure was refined with a full matrix-squares algorithm minimizing the function $\Sigma w(F_o - F_c)^2$. Refinement including anisotropic thermal parameters for all atoms and a parameter accounting for secondary extinction converged to final residuals of $R = 0.0536$ and $R_w = 0.0574$. Analysis of $\Sigma w(F_o - F_c)^2$ as a function of Miller indices, F_o^2, $\sin\theta/\lambda$ and setting angles showed no unusual trends. Detailed information concerning the structure analysis is given in Table 1. The final positional and equivalent isotropic thermal parameters are listed in Table 2. Further details concerning the structure determination are available on request from the Fachinformationszentrum Karlsruhe GmbH, D-76344 Eggenstein-Leopoldshafen, by quoting the depository number CSD-59001, the names of the authors, and the journal citation.

Table 2. Positional parameters and U_{eq} values[a] [Å^2] for Ta_4FeTe_4

Atom	site	*x/a*	*y/b*	*z/c*	U_{eq}
Ta(1)	4g	0.0687(2)	0.1196(1)	0	0.0167(5)
Ta(2)	4h	0.1972(2)	0.0578(1)	1/2	0.0170(5)
Ta(3)	4g	0.2107(2)	0.9615(1)	0	0.0171(5)
Ta(4)	4h	0.8998(2)	0.1119(1)	1/2	0.0168(5)
Te(1)	4g	0.3382(2)	0.0986(2)	0	0.0201(9)
Te(2)	4h	0.3593(2)	0.9327(2)	1/2	0.0194(8)
Te(3)	4h	0.1146(3)	0.2059(2)	1/2	0.0201(9)
Te(4)	4g	0.8300(3)	0.1915(2)	0	0.0200(9)
Fe	4e	0	0	0.251(1)	0.020(2)

[a] Equivalent isotropic U_{eq} defined as one third of the trace of the orthogonalized U_{ij} tensor.

Electrical Resistivity Measurements: All manipulations were carried out under a continuous flow of argon. A needle-shaped crystal of Ta_4FeTe_4 (approximate dimensions: 0.010 × 0.010 × 1.0 mm) was mounted on a microscope slide and two gold leads were attached to the crystal at both ends of the needle by using molten indium metal. The resistivity was measured as a function of temperature in the range from 275 K to 8 K and reverse at increments of 2 K. The absolute values of resistivity are only approximate due to difficulties in measuring the crystal dimensions accurately.

[1] J. A. Wilson, F. J. DiSalvo, S. Mahajan, *Adv. Phys.* **1975**, *24*, 117; *Crystal Chemistry and Properties of Materials with Quasi One-Dimensional Structures* (ed.: J. Rouxel), Reidel, Dordrecht, **1986**; *Electronic Properties of Inorganic Quasi One-Dimensional Compounds*; Part 1 and 2 (ed.: P. Monceau), Reidel, Dordrecht, **1985**; *Theoretical Aspects of Band Structures and Electronic Properties of Pseudo One-Dimensional Solids* (ed.: H. Kamimura), Reidel, Dordrecht, **1985**.

[2] J. A. Wilson, A. D. Yoffe, *Adv. Phys.* **1969**, *18*, 193.

[3] R. H. Friend, A. D. Yoffe, *Adv. Phys.* **1987**, *36*, 1; J. Rouxel, R. Brec, *Ann. Rev. Mater Sci.* **1986**, *16*, 137; *Intercalation Chemistry* (Eds.: M. S. Wittingham, A. J. Jacobson), Academic Press, New York; **1982**; F. Hulliger in *Physics and Chemistry of Materials with Layered Structures, Vol. 5; Structural Chemistry of Layer-Type Phases* (ed.: F. Lévy), Reidel, Dordrecht, **1976**.

[4] R. Chevrel, M. Sergent, J. Prigent, *J. Solid State Chem.* **1971**, *3*, 515.

[5] K. Yvon, *Curr. Top. Mater. Sci.*, **1979**, *3*, 53; R. Chevrel in: *Superconductor Materials Science*, Chapter 10 (eds.: S. Flomer,

B. B. Schwartz) Plenum, New York, **1981**, O. Fischer, *Appl. Phys.* **1978**, *16*, 1.
[6] W. Hönle, H. G. von Schnering, A. Lipka, K. Yvon, *J. Less-Common Met.* **1980**, *71*, 135; M. Potel, R. Chevrel, M. Sergent, J. C. Armici, M. Decroux, O. Fischer, *J. Solid State Chem.* **1980**, *35*, 286; M. Potel, R. Chevrel, M. Sergent, *Acta Chystallogr.* **1980**, *B36*, 1545; J. Huster, G. Schippers, W. Bronger, *J. Less-Common Met.* **1988**, *91*, 333.
[7] B. Harbrecht, H. F. Franzen, *J. Less-Common Met.* **1985**, *113*, 349; B. Harbrecht, *J. Less-Common Met.* **1986**, *124*, 125.
[8] B. Harbrecht, *J. Less-Common Met.* **1988**, *141*, 59; K. Ahn, T. Hughbank, *J. Solid State Chem.* **1993**, *102*, 446.
[9] H. F. Franzen, J. G. Smeggil, *Acta Crystallogr.* **1970**, *B26*, 125; B. Harbrecht, *J. Less-Common Met.* **1988**, *138*, 225.
[10] H. F. Franzen, J. G. Smeggil, *Acta Crystallogr.* **1969**, *B25*, 1736.
[11] S.-J. Kim, K. S. Nanjundaswamy, T. Hughbanks, *Inorg. Chem.* *1991*, *30*, 159.
[12] M. E. Badding, F. J. Disalvo, *Inorg. Chem.* **1990**, *29*, 3952.
[13] J. Li, R. Hoffmann, M. E. Badding, F. J. Disalvo, *Inorg. Chem.* **1990**, *29*, 3943.
[14] K. Ahn, T. Hughbanks, K. D. D. Rathnayaka, D. G. Naugle, *Chem. Mater.* **1994**, *6*, 418.
[15] B. E. Brown, *Acta Crystallogr.* **1966**, *20*, 264.
[16] J. Neuhausen, E. Potthoff, W. Tremel, J. Ensling, P. Gütlich, *Z. Naturforsch.* **1993**, *48b*, 797.
[17] *CRC Handbook of Chemistry and Physics,* 65th edition, CRC Press, Boca Raton, Fla, **1984**.
[18] J. Neuhausen, K.-L. Storck, E. Potthoff, W. Tremel, *Z. Naturforsch.* **1992**, *47b*, 1203.
[19] S. C. Lee, R. H. Holm, *J. Am. Chem. Soc.* **1990**, *112*, 9654.
[20] W. Bronger, M. Kimpel, D. Schmitz, *Angew. Chem.* **1982**, *94*, 562; *Angew. Chem. Int. Ed. Engl.* **1982**, *21*, 544; W. Bronger, M. Kimpel, D. Schmitz, *Acta Crystallogr.* **1983**, *B39*, 235.
[21] M. L. Steigerwald, T. Siegrist, S. M. Stuczynski, Y.-U. Kwon, *J. Am. Chem. Soc.* **1992**, *114*, 3155; F. Cecconi, C. A. Ghilardi, S. Midolini, A. Orlandini, *J. Chem. Soc. Chem. Commun.* **1992**, 910.
[22] J. Neuhausen, W. Tremel, *J. Alloys Compd.* **1994**, *204*, 215.
[23] A. Simon, *Angew. Chem.* **1988**, *100*, 163; *Angew. Chem. Int. Ed. Engl.* **1988**, *27*, 159.
[24] A. Simon, H. G. von Schnering, H. Wöhrle, H. Schäfer, *Z. Anorg. Allg. Chem.* **1965**, *339*, 155.
[25] D. Bauer, H. G. von Schnering, *Z. Anorg. Allg. Chem.* **1968**, *361*, 259.
[26] J. Köhler, G. Svensson, A. Simon, *Angew. Chem.* **1992**, *104*, 1463; *Angew. Chem. Int. Ed. Engl.* **1992**, *31*, 1437. A. Simon in: *Clusters and Colloids,* Chapter 5 (ed.: G. Schmid), Verlag Chemie, Weinheim, **1994** and references cited therein.
[27] H. Kleinke, W. Tremel, submitted for publication in *Angew. Chem.*
[28] R. Chevrel, P. Gougeon, M. Potel, M. Sergent, *J. Solid State Chem.* **1985**, *57*, 25.
[29] H. Kleinke, W. Tremel, manuscript in preparation.
[30] W. Tremel, *J. Chem. Soc. Chem. Commun.* **1992**, 709.
[31] K. Yvon, W. Jeitschko, E. Parthé, *J. Appl. Crystallogr.* **1977**, *10*, 73.
[32] *International Tables for X-Ray Crystallography,* Vol. IV (eds.: J. A. Ibers, W. C. Hamilton), Kynoch Press, Birmingham, **1974**.
[345/94]